WINDS OF HOT STARS AS A DIAGNOSTIC TOOL OF STELLAR EVOLUTION

R.P. Kudritzki, A. Pauldrach, J. Puls
Institut für Astronomie und Astrophysik der Universität München
Scheinerstr. 1, D-8000 München 80

I. INTRODUCTION

Modern quantitative spectroscopy of hot stars has two aspects: the analysis of photospheric lines and stellar wind lines. The first one is meanwhile established as an almost classical tool to determine stellar parameters. NLTE model atmosphere and line formation calculations yield T_{eff}, log g and abundances with high precision (see recent reviews by Husfeld (this meeting), Kudritzki (1987), Kudritzki and Hummer (1986), Kudritzki, (1985)). The second aspect, however, the quantitative analysis of stellar wind lines is still at its very beginning. For long time the stellar wind lines have been used to determine mass-loss rates $\dot{M}$ and terminal velocities v_∞ only. While these studies were pioneering and of enormous importance, it was also clear that very approximate calculations were done with respect to NLTE ionization and excitation and the radiative transfer in stellar winds. Thus, stellar wind lines could be used only in a more qualitative comparative sense, with no theory behind, which allowed the determination of precise and reliable numbers.

However, during the past few years the situation has dramatically changed. The theory of radiation driven winds has been strongly improved and very detailed and complex multi-level NLTE calculations for stellar winds have become available. The purpose of this paper therefore is to convince that on the basis of this new framework stellar wind lines provide a powerful quantitative diagnostic tool to determine independently radii, luminosities and masses of stars.

II. THE THEORY OF RADIATION DRIVEN WINDS

Hot stars have an intense radiation field, which by absorption due to UV metal lines leads to an outward accelerating force, which is undoubtedly present. Lucy and Solomon (1970) and Abbott (1979) proved convincingly that this radiation force is sufficient to initialize and to maintain stellar winds. The domain of self-initializing winds predicted by the theory coincides almost perfectly with the occurence of mass-loss in the upper left part of the HR-diagram (see Abbott,

https://doi.org/10.1017/S025292110009357X Published online by Cambridge University Press

1979). Thus, we can conclude that winds of stars more massive than 20 $M_\odot$ are basically radiation driven.

The basic dynamical wind quantities are M and v_∞. What does the theory predict with respect to their dependence on the stellar parameters? This has been investigated in the pioneering paper by Castor, Abbott, Klein (1975, "CAK"), who for the first time formulated the theory of radiation driven winds in a selfconsistent way. Besides some crucial simplifying assumptions (see below) the theory in its later version (Abbott, 1982) used a realistic line list of 250000 lines of H to Zn in ionization stages I to VI. The prediction of the theory were:

$$\begin{aligned} - v_\infty &= (\alpha/1-\alpha)^{1/2} \; v_{esc} \\ - M &\sim L^{1/\alpha} (M(1-L/L_E))^{1-1/\alpha} \end{aligned} \qquad (1)$$

where the parameter α comes out as the result of the theory and lies between 0.5 and 0.7. As shown in Fig. 1, the predicted proportionality are roughly reproduced by the observations. However, with respect to the proportionality constants the old CAK theory fails. Predicted mass-loss rates are too high by a factor of three (Fig. 2a) and theoretical terminal velocities are too low by a large factor (Fig. 2). Since v_∞ can be measured with high precision from the blue edges of the velocity affected line profiles, the latter discrepancy cast enormous doubts on the theory.

However, recently Pauldrach, Puls and Kudritzki (1986, "PPK") were able to prove that this failure of the theory was caused by one of the crucial approximations made by CAK, namely the "radial streaming approximation". In this approximation the interaction of photospheric photons with the wind plasma is treated as if they were streaming out radially from the stellar surface. This approximation is very poor. Even some stellar radii away from the star the photosphere forms a finite cone angle (Fig. 3), which is crucial for correct treatment of momentum exchange. This "finite cone angle effect" was taken into account by PPK by introducing a correction factor CF to the CAK radiative force f^{CAK}.

$$f^{PPK} = CF \; f^{CAK}, \qquad CF = \frac{2}{1-\mu_*^2} \int_{\mu_*}^{1} \left(\frac{\mu^2 \, dv/dr + (1-\mu^2) \, v/r}{dv/dr}\right)^\alpha \mu d\mu \qquad (2).$$

Fig. 4 shows that CF<1 close to stellar surface. As a result M, which is fixed at the critical point close to the stellar surface is significantly reduced. Away from the star we have CF>1. In addition, due to

https://doi.org/10.1017/S025292110009357X Published online by Cambridge University Press

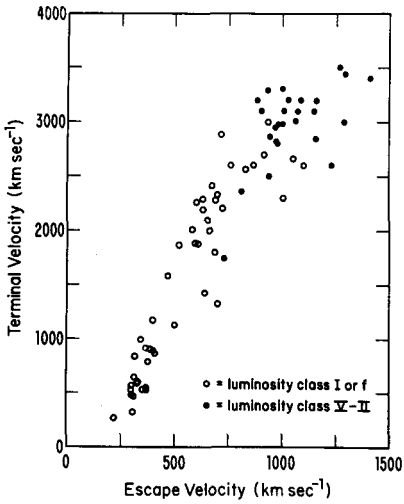

Fig. 1a: The observed relation between terminal velocity v_∞ and photospheric escape velocity v_{esc} (from Abbott, 1982).

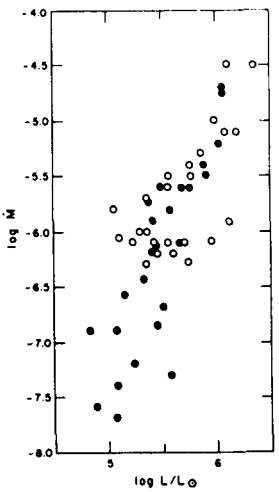

Fig. 1b: The observed relation of log $\dot{M}$ vs. log L, which obeys roughly $\dot{M} \sim L^{1.6}$ (from Garmany and Conti, 1984).

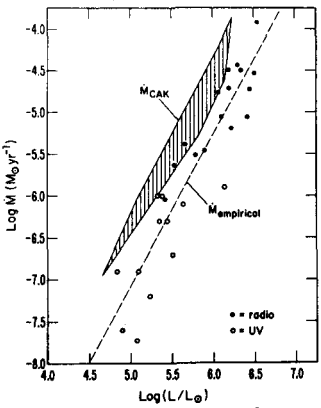

Fig. 2a: Observed log $\dot{M}$ vs. log L (dots) compared with predictions of CAK-theory (hatched area) (from Abbott, 1982).

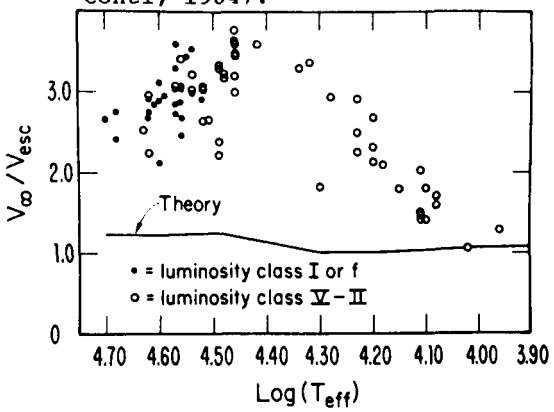

Fig. 2b: v_∞/v_{esc} as function of T_{eff} for individual stars compared with predictions of CAK-theory (from Abbott, 1982).

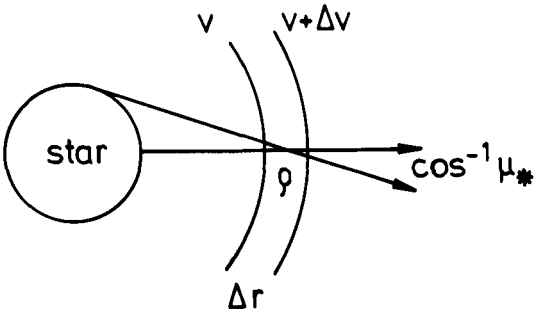

Fig. 3: The photospheric finite cone angle irradiating the expanding stellar wind shell.

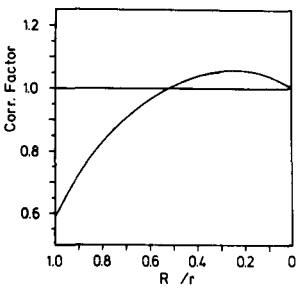

Fig. 4: Finite cone angle correction factor to the radiative force as function of reciprocal radius (from Pauldrach et al., 1986).

https://doi.org/10.1017/S025292110009357X Published online by Cambridge University Press

the lower $\dot{M}$ the wind density ρ is reduced in these outer layers (relative to the CAK case) and therefore - since $dv^2/dr \approx f/\rho$ - the wind material is much stronger accelerated. Consequently much higher values of v_∞ are obtained. (Similarly results were independently obtained in a recent paper by Friend and Abbott, 1987).

PPK have applied this improved wind theory on a sample of massive OB-stars with well determined wind properties. The results are given in Table 1 and show for given stellar parameters the observed dynamical wind quantities $\dot{M}$ and v_∞ are well reproduced by the theory. This includes even such extreme objects like P Cygni, which has an extremely high mass-loss rate and a very slow wind. The dynamically improved theory of radiation driven winds therefore appears to be highly reliable.

Table 1

star	spec.type	T_{eff} (10^3K)	log g (cgs)	log $L/L_\odot$	$\dot{M}_{obs}$ $10^{-6}M_\odot$/yr	$\dot{M}_{calc}$	v_∞^{obs} km/s	v_∞^{obs}
P Cyg	BIIa	18.0	2.0	5.64	20-30	29	400	395
ε Ori	B0Ia	28.5	3.25	5.91	3.1	3.3	2010	1950
ζ Ori	O9.5I	30.0	3.45	5.79	2.3	1.9	2290	2274
9 Sgr	O4(f)V	50.0	4.10	5.95	4.0	4.0	3440	3480
HD 48099	O6.5V	39.0	4.00	5.40	0.63	0.64	3500	3540
HD 42088	O6.5V	40.0	4.05	4.89	0.13	0.20	2600	2600
λ Cep	O6ef	42.0	3.7	5.90	4.0	5.1	2500	2500

III. THE EVOLUTION OF MASSIVE STARS AND THE DYNAMICS OF STELLAR WINDS

The observed terminal velocities v_∞ of O-stars provide interesting information about the evolution of massive stars. This is shown in Fig. 5, which is taken from Garmany and Conti (1985) and displays v_∞ vs. T_{eff} for a sample of O-stars (luminosity classes between V and III) in the Galaxy, LMC and SMC. Two striking facts can be read off from Fig. 5:

- the values of v_∞ form an inclined band vs. T_{eff}
- the values for LMC and SMC are on the average 500 km/s and 800 km/s deeper than for the Galaxy.

Kudritzki et al. (1987 "KPP") were able to explain both effects in terms of the improved theory of radiation driven winds. They calculated wind models for LMC, SMC and Galaxy using the reduced metal abun-

https://doi.org/10.1017/S025292110009357X Published online by Cambridge University Press

dances for the Clouds

$$Z_{LMC} = 0.28\ Z_{Gal}; \qquad Z_{SMC} = 0.1\ Z_{Gal}$$

as indicated by the analysis of the HII-region emission line spectra (Dufour, 1984). Table 2 contains the results for a typical O5V star:

Table 2: Calculated wind parameters for a typical O5V-star in Galaxy, LMC, SMC.

	v_∞ km/s	$\dot{M}$ $10^{-6} M_\odot/yr$	$\frac{\dot{M} v_\infty c}{L}$
Z_{Gal}	3350	2.12	0.66
Z_{LMC}	2900	1.35	0.36
Z_{SMC}	2435	0.72	0.16

Obviously, both v_∞ and $\dot{M}$ are significantly reduced by the lower metallicity. The effect on v_∞ is of the same order as it is observed, whereas the change in $\dot{M}$ is on the margin to be detectable.

In a next step KPP calculated wind models along evolutionary tracks of O-stars in all three galaxies. The tracks used the same metallicities as above and were calculated by Pylyser et al. (1985). Fig. 6 comprises the major results. The upper part contains simply the evolutionary tracks. However, contrary to the common HR-diagram v_{esc}, the escape velocity from the stellar surface, is plotted as function of T_{eff}. This "alternative HR-diagram" reveals that during the massive star evolution the v_{esc} values lie within an inclined band of the diagram. When the stars evolve away from the ZAMS, their radii increase and consequently their v_{esc} decrease. However, due to convective mixing, overshooting and mass-loss of the evolution turns back to the blue at roughly constant luminosity. This means that the radii decrease again. However, v_{esc} while mildly increasing does not approach the old values at the ZAMS, since the stars have now already lost a significant fraction of their mass.

In radiation driven wind theory v_∞ is related to v_{esc}. Thus we expect v_∞ to form a similar inclined band as v_{esc}. This is shown in the lower part of Fig. 6 together with the observed position of massive stars from Fig. 5. The agreement between theory and observation is obvious. We wish to point out here that diagrams of this type also allow to read of present stellar parameters and thus - at least in principle - provide an interesting alternative to the HR-diagram.

https://doi.org/10.1017/S025292110009357X Published online by Cambridge University Press

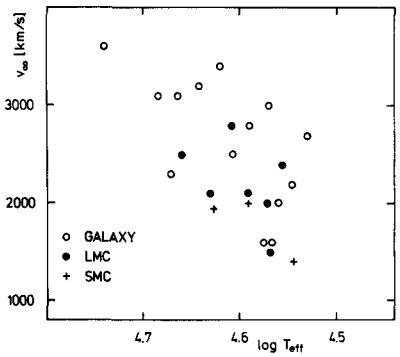

Fig. 5: Observed correlation of v_∞ vs. T_{eff} for O-stars in Galaxy, LMC and SMC (from Garmany and Conti, 1985).

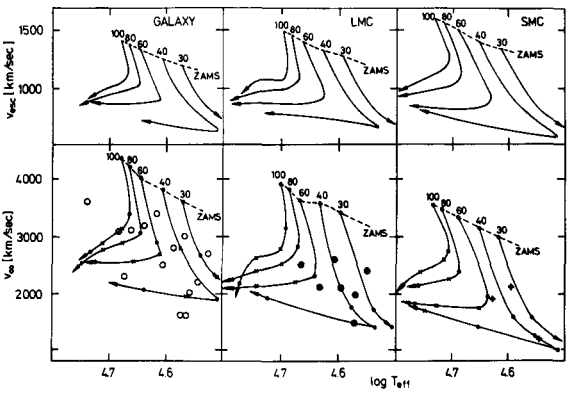

Fig. 6: The "alternative HR-diagram" of massive star evolution. Upper part: Surface escape velocity vs. T_{eff}. Lower part: Terminal veolcity vs. T_{eff}. The position of observed objects (see Fig. 5) is also shown.

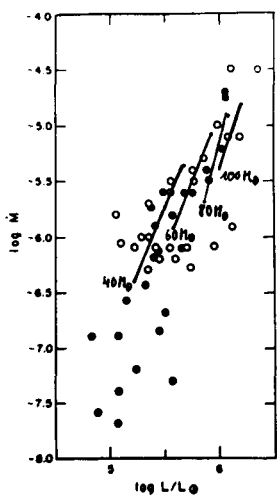

Fig. 9: The observed log L, log $\dot{M}$ relation for galactic O-stars (same as Fig. 16) compared with the theoretical results of Fig. 8.

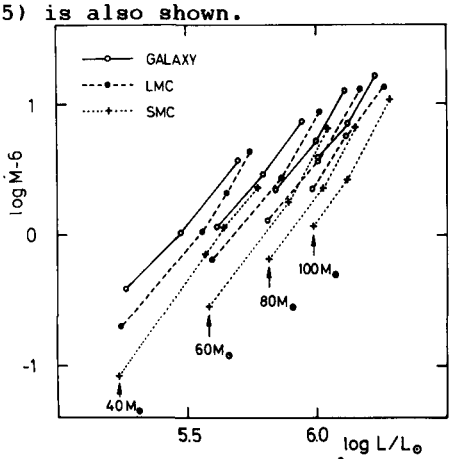

Fig. 8: The log L, log $\dot{M}$ relation along the evolutionary tracks as predicted by radiation driven wind theory.

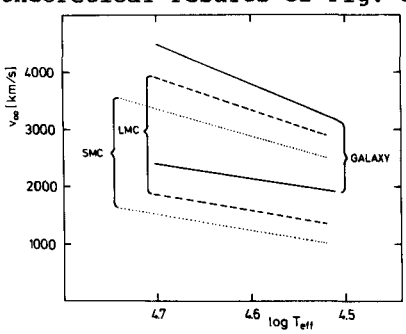

Fig. 7: The (v_∞, log T_{eff})-bands for each galaxy as obtained from the theoretical calculations of Fig. 6.

https://doi.org/10.1017/S025292110009357X Published online by Cambridge University Press

Fig. 7 shows the envelopes of the v_∞ vs. log T_{eff} tracks for each galaxy plotted into one diagram. Obviously the theory predicts the range of velocities in the Galaxy to lie above the LMC and the SMC. This agrees well with the observed effect in Fig. 5.

Fig. 8 displays the relation of log $\dot{M}$ vs. log L along the evolutionary tracks in each galaxy. It is clearly seen that for each track of similar initial mass the relation $\dot{M}_{Gal} > \dot{M}_{LMC} > \dot{M}_{SMC}$ holds. However, it will be hard to disentangle this effect observationally since the tracks cross each other at higher luminosity. Careful determination of stellar parameters based on detailed photospheric NLTE spectroscopy will be needed for this. (A comparison with observations of stars in our own galaxy is shown in Fig. 9).

Generally, we conclude that the theory of radiation driven winds describes the observed wind dynamics satisfactory. This includes also the dependence on metallicity.

IV. THE EVOLUTION OF MASSIVE STARS AND THE MORPHOLOGY OF STELLAR WIND SPECTRA

From the work by Walborn and collaborators (Walborn and Panek, 1984a,b, 1985; Walborn and Nichols-Bohlin, 1987; Walborn et al., 1985) it became evident that the appearance of stellar wind spectra shows systematic dependence on luminosity, effective temperature and abundance. It is of course crucial for a reliable stellar wind theory to reproduce these effects. This requires, however, detailed and very refined NLTE calculations for excitation and ionization in the winds of hot stars. For a long period such calculations were carried out in a very approximative way, until just very recently the first realistic calculations became available: Pauldrach (1987) adopted a cool wind ($T_W \approx T_{eff}$) and treated the full multi-level NLTE problem of all relevant elements and ions including electron collisions selfconsistently with the radiation driven wind hydrodynamics. He includes in total 26 elements , 133 ionization stages, 4000 levels, 10000 radiative bound-bound transitions in the rate quations and the ocrrect continuous radiation field for the bound-free rates calculated from the spherical transfer equation. Puls (1987) extended these improvements significantly further by including the "multi-line effects", which arise from the velocity induced line overlap, which causes radiative coupling between different ions and possible multiple momentum transfer from photons to the wind plasma. The first application of

https://doi.org/10.1017/S025292110009357X Published online by Cambridge University Press

this strongly improved theory on the case of the O4f-star ζ Puppis shows excellent agreement with respect to the dynamical quantities $\dot{M}$ and v_∞. In addition - and this is the really important result - an enormous shift towards higher ionization stages is obtained due to the detailed NLTE treatment. Thus, it was for the first time possible to reproduce by cool wind models the observed high ionization features of OVI, NV, CIV etc. A typical example is given in Fig. 10, which shows how perfectly the observed NV profile in the UV-spectrum of ζ Puppis can be reproduced by the selfconsistent radiation driven NLTE wind model atmospheres. Note that this is not a profile fit, where $\dot{M}$ and v(r) have been properly adjusted. It is the result of a selfconsistent calculation, which depends only on the choice of the stellar parameters log L/L_o, T_{eff} and log g.

We have now applied calculations of this type along evolutionary tracks for massive stars to investigate whether our wind models do also reproduce the change of spectral morphology during stellar evolution. Fig. 11 displays the investigated parameter domain. Fig. 12 demonstrates the extreme behaviour of the SiIV resonance lines, which exhibit a pronounced luminosity effect both in theory and observation. The physical reason for this effect, which will prove to be of enormous potential for the luminosity classification of extragalactic O-stars using HST, is that in the winds of O-stars most of the silicon is SiV. Supergiants are closer to the Eddington limit and thus according to eq. (1) have denser winds, which leads to stronger recombination towards SiIV. Consequently, the SiIV wind features show up in the supergiants. The behaviour of NV, NIV, CIV can also be reproduced by the models, but this is not shown here for sake of brevity.

The improved stellar wind models are obviously able to describe the observed changes of spectral morphology as function of T_{eff} and L in a proper way. This - after a phase of calibration by detailed quantitative star by star spectral analysis of standards - will render the possiblity to use the ultraviolet wind spectra of hot stars for direct luminosity determination.

V. STELLAR WINDS AND THE EVOLUTION OF CENTRAL STARS OF PN

After the advent of the IUE satellite it became undoubtedly clear that stellar winds are also present in many CSPN (Heap, 1978; Perinotto, 1982). Detailed studies of their wind properties have been carried out by Hamann et al. (1984) and Cerruti-Sola and Perinotto (1985). Here we

https://doi.org/10.1017/S025292110009357X Published online by Cambridge University Press

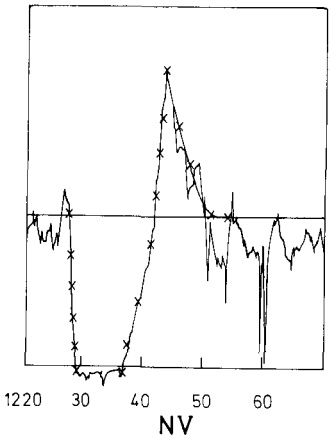

Fig. 10: The IUE high resolution profile of NV λ 1240 of ζ Puppis compared with the result from a selfconsistent radiation driven wind model (crosses), which includes full NLTE in all ions and multi line effects (from Puls, 1987).

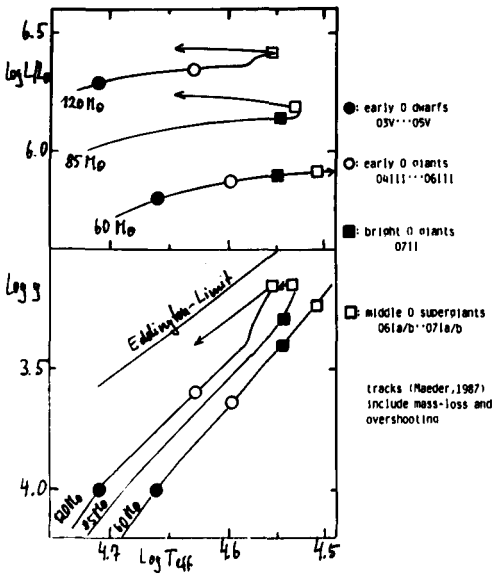

Fig. 11: Wind models along evolutionary tracks representing different luminosity classes.

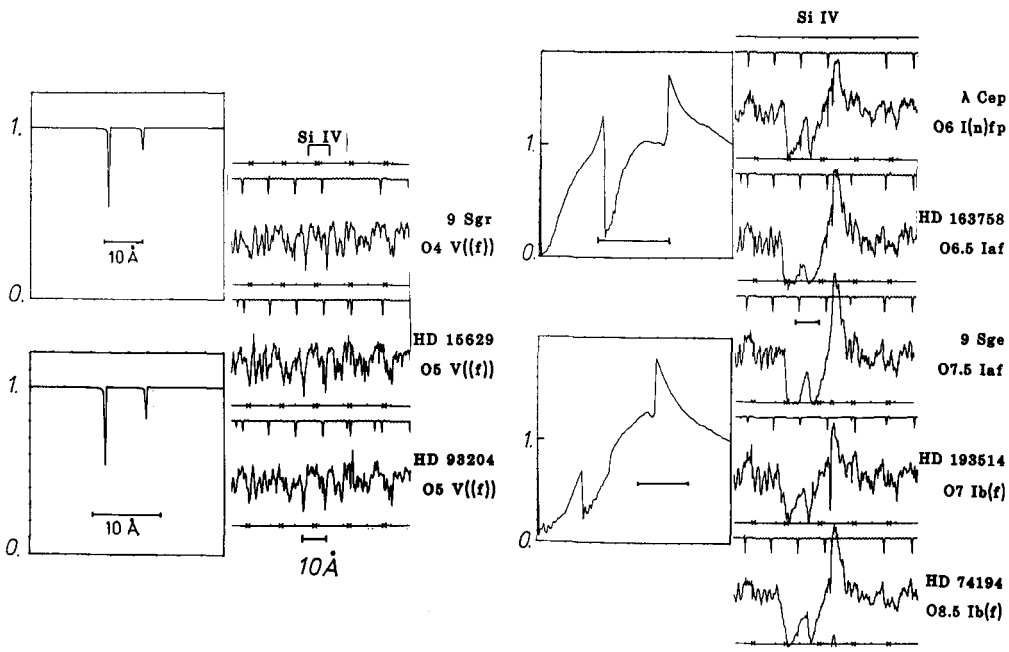

Fig. 12: The strong observed luminosity effect of SiIV as reproduced by the wind models. The observations are copied from Walborn et al. (1985). (For discussion see text).

https://doi.org/10.1017/S025292110009357X Published online by Cambridge University Press

want to concentrate on two striking observational correlations in the case of CSPN. The first one is displayed in Fig. 13, which exhibits the increase of terminal velocity with T_{eff}. Fig. 13 strongly points to radiation driven winds being present in the outer layers of CSPN, since in this case the terminal velocity is related to the surface escape velocity. CSPN evolve at constant luminosity towards the blue, so that the escape velocity increases. Consequently, we expect the terminal velocity to increase with T_{eff}.

The second observational correlation results from the detailed photospheric quantitative spectroscopy by Méndez et al. (1987), which allows to determine the position of CSPN in the log g, log T_{eff}-plane with high precision. By transformation of evolutionary tracks into this plane stellar masses M/M_o and radii R/R_o can be read off directly. The log g, log T_{eff} diagram of CSPN can also be used to investigate how the strength of stellar winds depends on the stellar parameters. This is done in Fig. 14, which reveals clearly that the more massive objects closer to the Eddington limit have observable wind features.

We have now applied our improved radiation driven wind theory also on wind models along post-AGB tracks by Schönberner (1983) and Wood and Faulkner (1986). Fig. 15 shows the calculated relation between terminal velocity and T_{eff} along the evolutionary tracks, including the observed values for CSPN. The result is extremely convincing. It again allows to read off stellar masses directly, and suggests that the masses of CSPN are in a rather narrow range between 0.5 and 0.8 solar masses (Schönberner, 1981; Méndez et al., 1985, 1987). This reveals the power of stellar wind models for the determination of stellar masses.

As indicated in Fig. 14 also the wind features in the optical spectra become significant at higher masses of the CSPN. This is demonstrated by Fig. 16, which shows how HeII 4686 switches from photospheric absorption into wind emission with increasing mass. It is important to test whether radiation driven wind models can reproduce this behaviour.

For this purpose, a new type of "unified model atmospheres" has been developed at the Munich Observatory by R. Gabler (1986) and A. Wagner (1986) in cooperation with J. Puls, A. Pauldrach and R.P. Kudritzki. These NLTE model atmospheres are spherically extended, in radiative equilibrium, and include the density and velocity distribution of radiation driven winds. The spectra of H and He lines are then calcu-

https://doi.org/10.1017/S025292110009357X Published online by Cambridge University Press

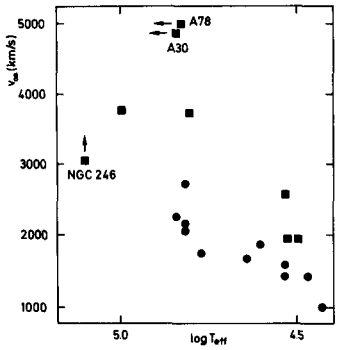

Fig. 13: Terminal velocity versus T_{eff} for CSPN. Squares are H-deficient objects; circels, normal Hydrogen abundance.

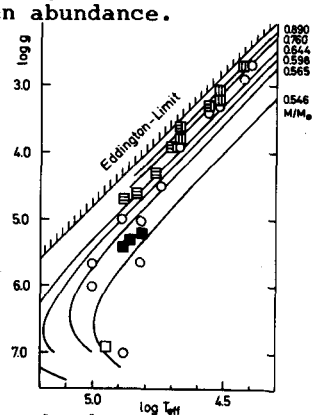

Fig. 14: The log g, log T_{eff} diagram of CSPN compared with post AGB-tracks. The presence of winds in the optical and for UV spectra is indicated as follows: IUE wind detections, wind detections by optical spectra, no winds in optical - no IUE high resolution spectra taken, objects with definitely no wind.

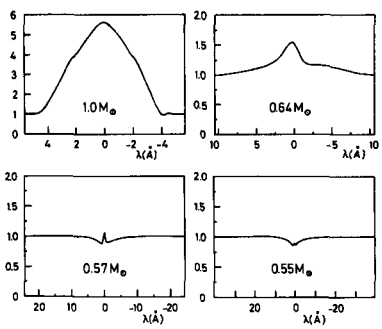

Fig. 18: HeII 4686 model profiles at T_{eff} = 50000K for different CSPN masses. Note the enormous emission at one solar mass.

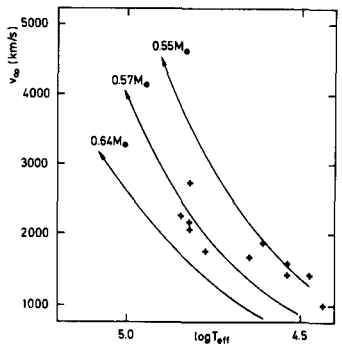

Fig. 15: Same as Fig. 13 for CSPN with normal H abundance, but including wind calculations along evolutionary tracks.

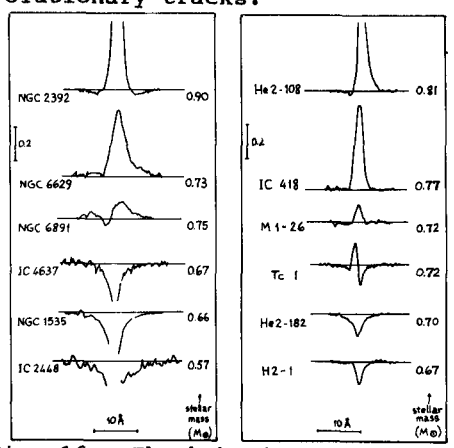

Fig. 16: The behaviour of the stellar HeII 4686 as a function of the stellar mass. The left and right panels are for objects with T_{eff} around 50000K and 35000K, respectively.

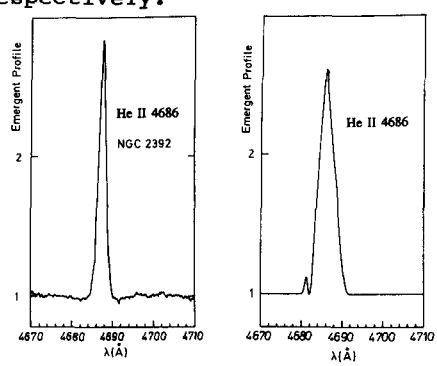

Fig. 17: The observed HeII 4686 profile of the high mass CSPN NGC 2392 (left) compared with a model calculation for one solar mass and T_{eff} = 45000K.

https://doi.org/10.1017/S025292110009357X Published online by Cambridge University Press

lated for these models by detailed NLTE multi-level calculations in the whole atmosphere, thus treating the contribution of subsonic deeper and supersonic outer layers to the emergent line profile in the correct self-consistent unified way, including Stark-effect broadening and velocity fields. We have calculated a sequence of such models for T_{eff} = 50000K and stellar masses equal to 0.55, 0.57, 0.64 and 1 solar masses. The corresponding luminosities of the CSPN (or the gravities or the radii) were obtained from the evolutionary tracks mentioned already in the previous section. In units of the Eddington luminosity L_E, we obtain, respectively, L/L_E = 0.06, 0.16, 0.34, 0.74. The more massive object is therefore already rather close to the Eddington limit. Its theoretical HeII 4686 profile should look similar to the one of the central star of NGC 2392, following Méndez et al. (1987). Fig. 17 shows that this is really the case. In addition, the turnover from photospheric absorption to wind emission with increasing L/L_E, as observed by Méndez et al., is well reproduced by the theoretical computations displayed in Fig. 18. This demonstrates that the concept of radiation driven winds is very useful also for CSPN. Moreover, it renders the possibility to use the 4686 emission as a powerful luminosity (=mass, =distance)-indicator. In future work this will be tested quantitatively.

ACKNOWLEDGEMENTS

This work was supported by the Deutsche Forschungsgemeinschaft under grants Ku 474/11-1 and Ku 474/13-1.

REFERENCES

Abbott, D.C.: 1979, IAU Symp. 83, p. 237
Abbott, D.C.: 1982, Astrophys. J. 259, 893
Castor, J., Abbott, D.C., Klein, R.: 1975, Astrophys. J. 195, 157
Cerruti-Sola, M., Perinotto, M.: 1985, Astrophys. J. 291, 237
Dufour, R.J.: 1984, IAU Symp. 108, p. 353
Friend, D., Abbott, D.C.: 1986, Astrophys. J. 311, 701
Gabler, R.: 1986, Diplomarbeit, Universität München
Hamann, W.R., Kudritzki, R.P., Méndez, R.H., Pottasch, S.R.: 1984, Astron. Astrophys. 139, 459
Heap, S.R.: 1978, IAU Symp. 83, p. 99
Kudritzki, R.P.: 1985, Proc. ESO Workshop on "Production and Distribution of C,N,O Elements", ed. J. Danziger et al., p. 277 (invited paper)

Kudritzki, R.P.: 1987, "Spectroscopic Constraints on the Evolution of Subluminous O-stars and Central Stars of PN", Proc. of IAU Coll. No. 95 on Faint Blue Stars, ed. Davis Philip, in press

Kudritzki, R.P., Hummer, D.G.: 1986, Proc. IAU Symp. 116, ed. de Loore et al., p. 3

Kudritzki, R.P., Pauldrach, A., Puls, J.: 1987, Astron. Astrophys. 173, 293

Lucy, L.B., Solomon, P.: 1970, Astrophys. J. 159, 879

Méndez, R.H., Kudritzki, R.P., Herrero, A., Husfeld, D., Groth, H.G.: 1987, Astron. Astrophys., in press

Méndez, R.H., Kudritzki, R.P., Simon, K.P.: 1985, Astron. Astrophys. 164, 86

Pauldrach, A.: 1987, Astron. Astrophys. 183, 295

Pauldrach, A., Puls, J., Kudritzki, R.P.: 1986, Astron. Astrophys, 164, 86

Perinotto, M.: 1982, IAU Symp. 103, p. 323

Puls, J.: 1987, Astron. Astrophys. 184, 227

Pylyser, E., Doom, C., de Loore, C.: 1985, Astron. Astrophys. 148, 379

Schönberner, D.: 1981, Astron. Astrophys. 103, 119

Schönberner, D.: 1983, Astrophys. J. 272, 708

Wagner, A.: 1986, Diplomarbeit, Universität München

Walborn, N.R., Panek, R.J.: 1984, Astrophys. J. 280, L27

Walborn, N.R., Panek, R.J.: 1984, Astrophys. J. 286, 718

Walborn, N.R., Panek, R.J.: 1985, Astrophys. J. 291, 806

Walborn, N.R., Nichols-Bohlin, J.: 1987, PASP 99, 40

Walborn, N.R., Nichols-Bohlin, J., Panek, R.J.: 1985, "IUE Atlas of O-Type Spectra from 1200 to 1900Å", NASA Reference Publication 1155

Wood, P.R., Faulkner, D.J.: 1986, Astrophys. J. 307, 659